Effect of addition of fillers on Cellulose/β-TCP polymer Composites: Thermal, Mechanical and Antimicrobial Properties

T. S. Kiruthika[1], B. Deepan Kumar[1,2] and V. Jaisankar[1]*
[1]PG and Research Department of Chemistry, Presidency College (Autonomous), Chennai-600 005, Tamil Nadu, India.
[2]Department of Chemistry, Institute of Chemical Technology, Tharamani, Chennai-600 113, Tamil Nadu, India.
*Email: vjaisankar@gmail.com

Received: 13.7.23 Revised: 25.8.23, 28.8.23,28.10.23 Accepted: 28.10.23

Abstract

Cellulose-based polymeric composites have received considerable attention as appealing biomimetic alternatives for a variety of biological applications because of their unique mechanical characteristics and appreciable bioactivity. In this investigation, four ternary polymeric composites were prepared, with cellulose serving as a typical common biopolymer and β-tricalcium phosphate (β-TCP) serving as a common bioceramic component. The naturally available hemp was used for the isolation of cellulose. The solution precipitation process was used to create the bioceramic substance β-TCP. Cellulose/Agar-Agar (AA)/β-TCP, Cellulose/*I*-Carrageenan (CC)/β-TCP, Cellulose/Polyvinyl alcohol (PVA)/β-TCP, and Cellulose/Polyvinylpyrrolidone (PVP)/β-TCP were the four polymeric composites prepared. The thermal and mechanical properties of the prepared composites were analysed and were compared. The SEM images of these materials indicated that the presence of β-TCP in the composites reveals notable morphological changes in the surface that are appropriate for the cell adhesion nature. The antimicrobial properties such as antibacterial, antifungal, anticancer and *in vitro* wound healing ability of the prepared composites open a new perspective in the applications for biomaterials field.

Key words: cellulose, hemp, mechanical, bioceramic, *in vitro*, wound healing.

1 Introduction

Polymer matrix composites (PMCs) have recently received a lot of attention in the scientific community due to their outstanding features that make them ideal for a wide range of technical applications. It is well recognized that composite materials are more affordable, easier to produce, and have improved strength and durability [1,2]. Due to the wide range of features of PMCs, current research focuses primarily on the production of PMCs reinforced with fibres (either natural or synthetic) and fillers (either organic or inorganic). Particularly,

 DOI: 10.59143/isas.jisas.2.2.NOQE5610

synthetic fibres are mainly favoured in marine, automotive, aerospace, and construction applications because of their better strength, heat retention, durability, performance with lightweight materials, cheap investment requirements, and capacity to manufacture any complex structure. In addition, natural fiber-reinforced polymer composites (FRP) are most frequently created and employed in a variety of structural and non-structural applications with low to medium loads. Natural fibre composites are light in weight, entirely recyclable, renewable, and sustainable. They also have cheap extraction and processing costs. Fibre content, fibre orientation, fibre size, and fibre placement are only a few of the factors that affect how natural fibre composites behave [3,4]. However, some flaws in natural and synthetic fibres meant that the obtained composites' qualities did not match what was anticipated. As a result, researchers discovered numerous strategies for enhancing the characteristics of FRPs. Generally speaking, two frequently used techniques (reinforcement of FRP and Hybridisation of FRP [26]) are used to enhance the mechanical, physical, thermal, tribological, and optical properties of FRPs.

The process of hybridising a composite involves combining FRPs with different kinds of natural or synthetic fibres or fillers to create composites that have the combined qualities of the two materials and may be used in a wider range of applications. If the fibres are hybridised, there are a variety of techniques one can use, such as layer-by-layer stacking, placing various fibres in a single layer, changing the orientation of the fibres, and placing only certain fibres in a layer. By including nanofillers, hybridization can be accomplished even at the nanoscale, producing hybrid nanocomposites [5,6]. The type of nanofiller used, how it was made, how it was dispersed, and how the fillers interacted with the fibres and matrix all affected the properties of hybrid nanocomposites. The incorporation of filler materials into a polymer matrix or FRPs is a frequent study topic pursued by a variety of researchers. Filler materials are typically added to FRPs to enhance the material performance by enhancing the physical and mechanical properties of the composites. They are generally thought of as inert materials. Fillers provide composites a better surface quality and delay the development of coarse structure, resulting in improved mechanical qualities that are hard to achieve with coarse structure [7,8]. Either organic or inorganic materials are used as fillers. To achieve improved thermal stability, tribological behaviour, good interfacial features, and higher mechanical qualities, inorganic fillers are utilized in polymer composites.

2 Experimental

2.1 Materials and Methods

The chemicals used in the isolation of cellulose and carboxymethyl cellulose were Sodium hydroxide, Hydrogen peroxide, sodium metabisulphide, Glacial acetic acid, Ethanol, Hydrochloric acid, Monochloroacetic acid and Methanol were purchased from Alfa Aesar. The chemicals used for the preparation of bioceramics β-Tricalcium phosphate were Calcium nitrate tetrahydrate (CNT), Phosphoric acid, Ammonia, Potassium dihydrogen phosphate and were purchased from Alfa Aesar [17,18]. All the aqueous solutions used in the preparation were made with distilled water. The Analar grade solvents used in the investigation were purchased from Merck.

2.2 Isolation of Cellulose from hemp

The cellulose has been isolated from various plant sources namely hemp, jack fruit peel, pineapple leaves and corn cobs. The yield of cellulose isolated from hemp was high and possess optimal physico-chemical properties [19]. Hence, it is chosen for the preparation of cellulose composites, characterisation and biomedical applications.

2.3 Synthesis of β-Tricalcium phosphate

In the preparation, Calcium nitrate tetrahydrate (CNT) and Potassium dihydrogen phosphate were used as calcium and phosphorous precursors respectively. Aqueous solution of 1M calcium nitrate tetrahydrate and 0.67M potassium dihydrogen phosphate were prepared [20]. The prepared CNT solution was added slowly drop wise in a beaker containing potassium dihydrogen phosphate. Ammonia was added to maintain the pH 11 during the reaction and was kept in magnetic stirring for 1 h. Gelation started to occur and was kept aging for 24 h. The resulting filtrate was then rinsed with distilled water and was then subjected to calcination at 1000 °C for 30 min.

2.4 Preparation of polymer composites

The polymeric composite composed of cellulose/Agar-Agar (AA)/ β-TCP was prepared by solution casting method. The stoichiometric ratio of Cellulose:AA:β-TCP taken was 5:4:1 for the preparation. Initially, cellulose from hemp and Agar-Agar were dissolved in hot water separately and were mixed [24]. Then the mixture was stirred for about few hours. To this

desired amount of β-TCP powder, dissolved in distilled water was added. The mixture was stirred vigorously for 2 h and was cast on a teflon petri dish and was dried in an oven. Similarly, the polymer composites cellulose/AA/β-TCP, cellulose/CA/ β-TCP, Cellulose/PVA/β-TCP and cellulose/PVP/β-TCP were also prepared.

3 Results and Discussion

The β-TCP integrated cellulose composites were characterized by the following analytical techniques.

3.1 FTIR Spectral Analysis

The FTIR spectra for β-TCP, cellulose/AA/β-TCP, cellulose/CA/β-TCP, cellulose/PVA/β-TCP and cellulose/PVP/β-TCP are shown in Fig I. For β-TCP, the prominent absorption bands at 3443 and 1638 cm^{-1} are ascribed to adsorbed water [22, 23]. The PO_4^{3-} group is stretched in the bands at 900-1200 cm^{-1} [22,23]. The vibration peaks of PO_4^{3-} in β-TCP are shown by the strong peaks at 561 cm^{-1} and 607 cm^{-1}.

The IR absorption peaks for composites show the peak at 3429 cm^{-1} is for the OH stretching vibration whereas the peak at 2921 cm^{-1} is connected with methoxyl groups. The peak at 2852cm^{-1} is for the CH_2 bending vibration. The peak at 1633 cm^{-1} corresponds to the surface adsorbed water molecule. The peak at 1025 cm^{-1} is corresponds for the OH bending vibration and the peak at 847 cm^{-1} is for 3,6-anhydro-galactose bridges. The peaks at 562 cm^{-1} and 617 cm^{-1} is for the PO_4^{3-} groups in β-TCP. The peak at 2920 cm^{-1} corresponds to the stretching vibration of C-H group. The peat at 1731 cm^{-1} is for the C=O stretching vibration. The peak at 1428 cm^{-1} is for the CH_2 bending of pyranose ring. The peaks around 900 cm^{-1} - 1200 cm^{-1} is for the stretching mode of PO_4^{3-}. The peak at 1141 cm^{-1} is for the C-O-C stretching vibration. The peak at 670 cm^{-1} corresponds to the PO_4^{3-} vibration of tricalcium phosphate. The peak at 2919 cm^{-1} is for the Asymmetric stretching of pyrole ring. The peak at 2847 cm^{-1} corresponds to the CH stretching vibration. The peak at 1628 cm^{-1} is for the surface adsorbed water molecules of the tricalcium phosphate. The peak at 1453 cm^{-1} is for the CH_2 stretching vibration [16,19]. The peak at 1359 cm^{-1} is for the CH asymmetric deformation. The peak at 1220 cm^{-1} is for the stretching vibration of PO_4^{3-}. The peak at 914 cm^{-1} corresponds to the C-O-C stretching vibration. The vibrational peaks due to PO_4^{3-} are seen in the range of 561 - 607 cm^{-1}.

3.2 X-ray Diffraction Analysis (XRD)

The average crystallite size and average crystallinity index of the composites were calculated using Scherrer's formulae. The XRD spectra for cellulose/AA/β-TCP, cellulose/CA/β-TCP, cellulose/PVA/β-TCP, cellulose/PVP/β-TCP and β-TCP are shown in Fig 2. The distinctive peaks of AA, CA, PVA, and PVP appear in the diffraction patterns of the Cellulose/AA/β-TCP, Cellulose/CA/β-TCP, Cellulose/PVA/β-TCP and Cellulose/PVP/β-TCP composites after blending with cellulose and β-TCP [18,21]. When cellulose interacted substantially with the hydroxyl groups of Agar-Agar, Carragenan, PVA, and PVP, the percentage crystallinity of the composites increased [18,21]. The intensity of the peaks corresponding to the blend composites Cellulose/AA/β-TCP, Cellulose/CA/β-TCP, Cellulose/PVA/β-TCP and Cellulose/PVP/β-TCP are significantly lowered due to the enhanced diffraction of ceramic crystals or perhaps because the diffraction peaks of β-TCP overlap.

For the blend composite with β-TCP included, a reduced percentage of crystallinity is seen at 42%. The composites show two small, low-intensity 2θ peaks. The diffraction formed around the 2θ = 22.6, 22.05, 22.57, 22.08 representing the crystallographic planes of [111], [002] and [040] are in agreement with the JCPDS#030289 value of native cellulose [22].

The Crystallinity index (CI) and Average crystallite size (D) values of the samples are listed in Table 1. Accordingly, Cellulose/PVP/β-TCP composite shows low crystallinity index which may be due to its amorphous nature.

3.3 Thermal Analysis

To assess the thermal stability and comprehend the phase changes of the prepared samples, thermogravimetric (TG) and derivative thermogravimetric (DTG) studies were performed between 5 °C and 600 °C.

3.3 (a) Thermogravimetric analysis

The TGA thermograms for cellulose/AA/β-TCP, Cellulose/CA/β-TCP, Cellulose/PVA/β-TCP and cellulose/PVP/β-TCP are shown in fig III. For β-TCP, the first weight loss was observed at 250 °C – 350 °C [20,23]. The stability of β-TCP powders is proved by the lack of weight change after 600 °C**.** For cellulose/AA/β-TCP composite, the initial weight loss occurred up to 200 °C which is for the surface absorbed water molecules being about 45%.

The second weight loss was seen at 270 °C – 470 °C which corresponds to Agar-Agar and cellulose at 38%. The third weight loss was at 630 °C proving the decomposition of β-TCP which being about 13%. In cellulose/CA/β-TCP composite, the initial weight loss occurred at 90 °C is for the organic moiety and surface absorbed water molecule was about 35%. The second weight loss occurred at 1700 °C – 450 °C is for the *I*-carrageenan and cellulose with 42.94%. The third weight loss occurred at 500 °C which is for the decomposition of β-TCP with 13.49%.

In cellulose/PVA/β-TCP composite, the first weight loss occurred at 150°C which is for the organic moiety and surface absorbed water molecules. The second weight loss occurred at 350°C which is for the decomposition of PVA. The weight loss observed at 470 °C is for the decomposition of cellulose [19,20]. For cellulose/PVP/β-TCP composite, the initial weight loss occurred at 100 °C which is for the evaporation of water molecules and organic moiety. The second weight loss occurred between 210 °C – 450 °C which corresponds to the decomposition of cellulose. The third weight loss occurred at 440 °C - 550°C shows the decomposition of PVP. The fourth weight loss happened at 570°C showing the decomposition of β-TCP [21,22].

3.3 (b) Differential thermal analysis

DTA thermograms recorded are presented in Fig 4. For β-TCP, the initial endothermic zone ranges from 90°C to 295°C, with a peak at 250°C, corresponding to the dehydration of the precipitating complex and the loss of physically adsorbed water molecules in the hydroxyapatite powder. For Composites Cellulose/AA/β-TCP, a sharp exothermic peak was observed at 200°C. The loss of hydroxide from the cellulose and agar composite material is the cause of the release of heat by the sample during exothermic operations [18,19]. The results showed that the composites are thermally stable. For cellulose/CA/β-TCP composite also an exothermic peak was observed at 160°C, showing the released of heat by the sample during exothermic processes because of the loss of hydroxide from the cellulose and agar composite substance.

The thermal data shows that the composites are thermally stable for fabrication of bio composites materials for biomedical applications.

3.4 UTM analysis

The study of the mechanical properties of β-TCP composites and the correlation between the results have been discussed in UTM analysis. The mechanical responses to tension and strain in the separate β-TCP and cellulose based composites are normal [13,14]. The tensile strength of each polymer mixture was found to be significantly higher for thin film preparation.

It is evident from the table and Fig.5 that the cellulose/PVA/β-TCP composite exhibits greater elongation. The tensile characteristics of the combination materials were considerably better, as indicated in Table 3 [14,15]. It has also been suggested that incorporating bioceramics into polymer matrices enhances mechanical properties by creating potent interfacial contacts between the polymer strands and the surface of the bioceramics.

3.5 HR-SEM analysis

The scanning electron microscope is the most sophisticated tool for determining the minute details of the materials' microstructures [16,17]. To accurately portray the object's surface characteristics in relation to the sample's dimensions, SEM performs point-to-point scanning of the solid surface. The SEM images for β-TCP and β-TCP integrated cellulose based composites are shown in Fig 6.

The SEM images of β-TCP showed the rough outer surface which is due to the chemical treatment. For the composites cellulose/AA/β-TCP, cellulose/CA/β-TCP, cellulose/PVA/β-TCP and cellulose/PVP/β-TCP it is clearly seen that crystal shaped β-TCP particles are well dispersed in the composites and upon successive drying no agglomeration was found [18,19].

3.6 Energy Dispersive X-ray Spectroscopy

Using the EDX spectrum, the composition of polymer mixes and bioceramics was examined, and the findings are presented in Table 4 along with the composition's percentages.

Table 4 shows the percentage composition of the elements in the corresponding prepared composites.

3.7 Biomedical Evaluation

The use of morphologically regulated nanoparticles was crucial in adjustable antibacterial properties [24,25]. The creation of complex-shaped nanostructures with exact sizes is therefore

gaining popularity. It is well known that when bioceramic nanoparticles are embedded in a polymer matrix, they have a controlled and long-lasting discharge of particles in solution.

3.7.1 Antibacterial study

The results of the antibacterial studies obtained for four human pathogens against Cellulose/AA/β-TCP, Cellulose/CA/β-TCP, Cellulose/PVA/β-TCP, Cellulose/PVP/β-TCP prepared composites are given in Figs. 7 – 10.

3.7.1 (a) Antibacterial activity of cellulose/AA/β-TCP

The antibacterial activity of Cellulose/AA/β-TCP is shown in Fig 7.

From the zone of inhibition, it is observed that cellulose/AA/β-TCP composite is effective against *Enterococcus fecalis, Escherichia coli* and *Staphylococcus aureus*. Their Zone of inhibition values are in close agreement with the positive control.

3.7.1 (b) Antibacterial activity of cellulose/CA/β-TCP

The antibacterial activity of Cellulose/CA/β-TCP is shown in Fig 8.

From the zone of inhibition, it is observed that cellulose/CA/β-TCP composite is effective against *Enterococcus fecalis, Escherichia coli* and *Staphylococcus aureus*. Their Zone of inhibition values are in close agreement with the positive control.

3.7.1 (c) Antibacterial activity of cellulose/PVA/β-TCP

The antibacterial activity of Cellulose/PVA/β-TCP is shown in Fig 9.

From the zone of inhibition, it is observed that cellulose/PVA/β-TCP composite is effective against *Enterococcus fecalis, Escherichia coli* and *Staphylococcus aureus*. Their Zone of inhibition values are in close agreement with the positive control.

3.7.1 (d) Antibacterial activity of cellulose/PVP/β-TCP

The antibacterial activity of Cellulose/PV/β-TCP is shown in Figure 10.
From the zone of inhibition, it is observed that cellulose/PVP/β-TCP composite is effective against *Enterococcus fecalis, Escherichia coli* and *Staphylococcus aureus*. Their Zone of inhibition values are in close agreement with the positive control.

3.7.2 Antifungal activity

The results of the antifungal studies obtained for fungi against Cellulose/AA/β-TCP, Cellulose/CA/β-TCP, Cellulose/PVA/β-TCP, Cellulose/PVP/β-TCP prepared composites are given in the figs. 11 - 14 and tables 9 – 12.

3.7.2 (a) Antifungal activity of cellulose/AA/β-TCP

The antifungal activity of Cellulose/AA/β-TCP is shown in Fig. 11.

From the zone of inhibition, it is observed that cellulose/AA/β-TCP composite is effective against *Trichoderma viride, Candida albicans*. Their Zone of inhibition values are in close agreement with the positive control.

3.7.2 (b) Antifungal activity of cellulose/CA/β-TCP

The antibacterial activity of Cellulose/CA/β-TCP is shown in Fig 12.

From the zone of inhibition, it is observed that cellulose/CA/β-TCP composite is effective against *Trichoderma viride, Candida albicans, Rhizopus stolonifera*. Their Zone of inhibition values are in close agreement with the positive control.

3.7.2 (c) Antifungal activity of cellulose/PVA/β-TCP

The antifungal activity of Cellulose/CA/β-TCP is shown in Fig. 13

From the zone of inhibition, it is observed that cellulose/PVA/β-TCP composite is effective against *Trichoderma viride, Candida albicans*. Their Zone of inhibition values are in close agreement with the positive control.

3.7.2 (d) Antifungal activity of cellulose/PVP/β-TCP

The antifungal activity of Cellulose/PVP/β-TCP is shown in Fig. 14.

From the zone of inhibition, it is observed that cellulose/PVA/β-TCP composite is effective against *Trichoderma viride, Candida albicans*. Their Zone of inhibition values are in close agreement with the positive control.

3.7.3 Anticancer Activity

The anticancer activities of all the four composites were performed by MCF 7 cell lines. Measurements were performed and the concentration required for a 50% inhibition (IC_{50}) was determined graphically [22]. The percentage cell viability was calculated using the formulae,

% Cell viability = A570 of treated cells / A570 of control cells × 100

The cell viability percentage of the composites cellulose/AA/β-TCP, cellulose/CA/β-TCP, cellulose/PVA/β-TCP and cellulose/PVP/β-TCP are listed in Fig. 15

The above bar graph shows the anticancer activities of Cellulose/AA/β-TCP, Cellulose/CA/β-TCP, Cellulose/PVA/β-TCP and Cellulose/PVP/β-TCP composites. It clearly indicates that the cell viability % increases on decrease in concentration. From the comparative bar graph representation, Cellulose/PVA/β-TCP composites showed better activity than the other composites.

3.7.4 *In vitro* Wound healing

The wound healing test was performed using VERO cell types. The cells were inoculated into six-well dishes and left to incubate for 24 hours. After incubation, the cells were examined for development and a test was performed. Weighed samples were dissolved in DMSO [23,24]. A sample of 100g/ml was collected for examination. The medium was removed, and the dish was examined under a microscope. A sterile tip was used to make the incision. The well was filled with the appropriate quantity (100g/ml) and incubated. The dish was examined for cell development after 24 hours of incubation (Fig.16).

The wound closure percentage of the composites are listed below in the Table 13.

On comparing the wound closure percentage of the composites, Cellulose/PVA/β-TCP composite better activity than the other composites. The wound closure % was measured as 46.30%.

4 Conclusion

In this investigation cellulose/β-TCP based triblock composites were successfully prepared. The composites were characterized by FTIR, XRD and thermal analysis. The microstructure of polymer composites films was studied by SEM. The antimicrobial results showed that

these composites have optimal biomedical applications. The addition of filler significantly enhances the zone of inhibition in antibacterial and antifungal activities when compared to cellulose. Further it was observed that β-TCP composites have comparatively higher wound healing activity than the cellulose. Hence, the composites have vital applications in the medicinal field.

Acknowledgement

We would like to thank the Dr. Amirthavalli Raghupathy Memorial Fund for funding for our research laboratory.

Figures:

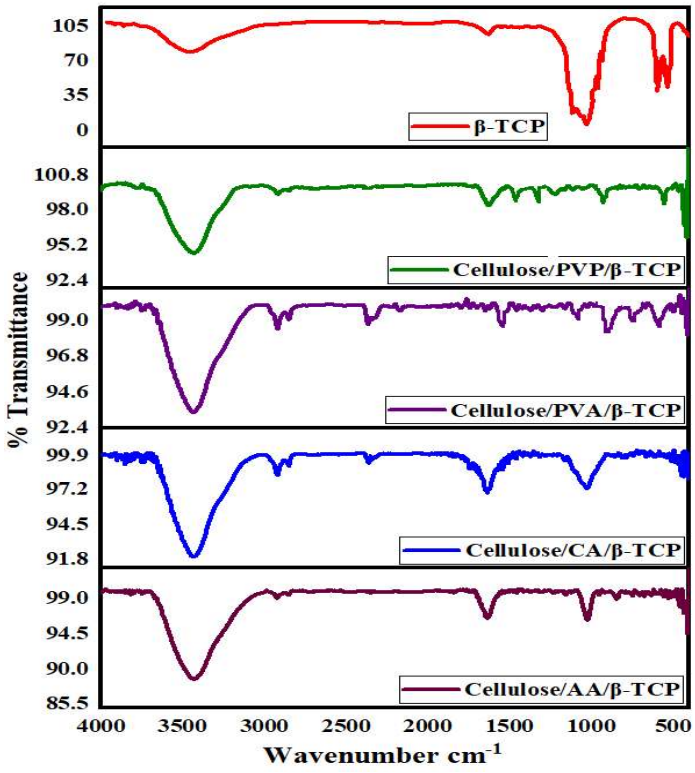

Fig. 1 FTIR spectra β-TCP and β-TCP integrated cellulose-based composites

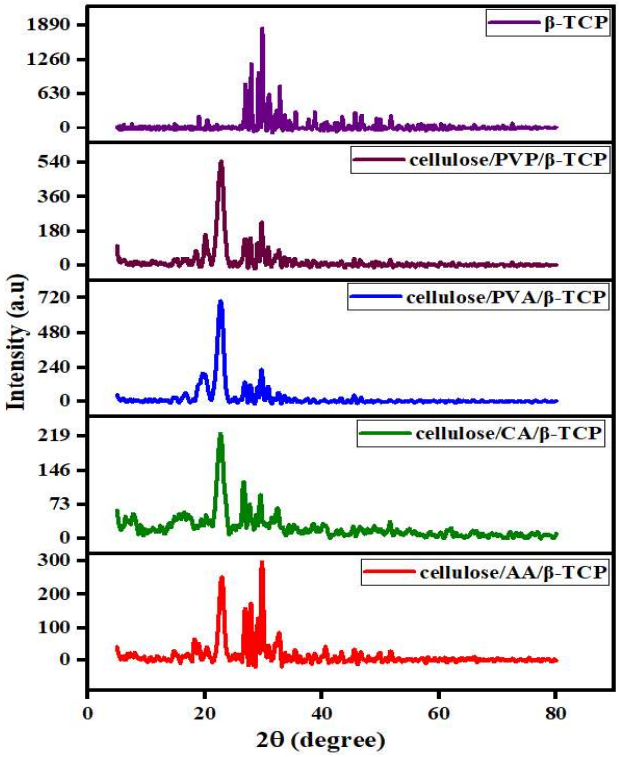

Fig. 2 XRD spectra β-TCP and β-TCP integrated cellulose based composites

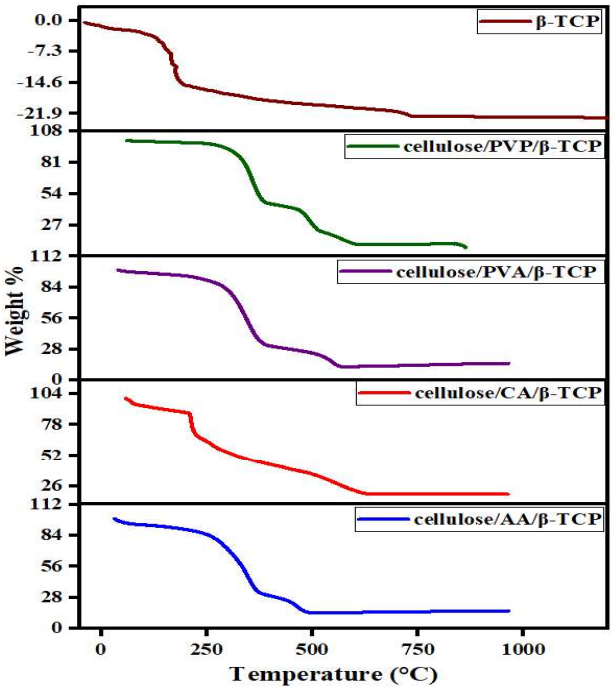

Fig. 3 TGA thermograms for β-TCP and β-TCP integrated cellulose based composites

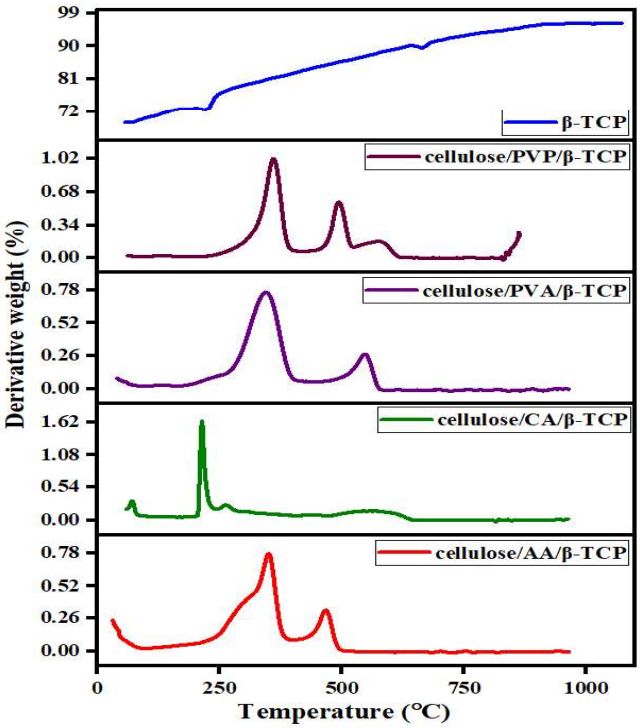

Fig. 4 DTA thermograms for β-TCP and β-TCP integrated cellulose based composites

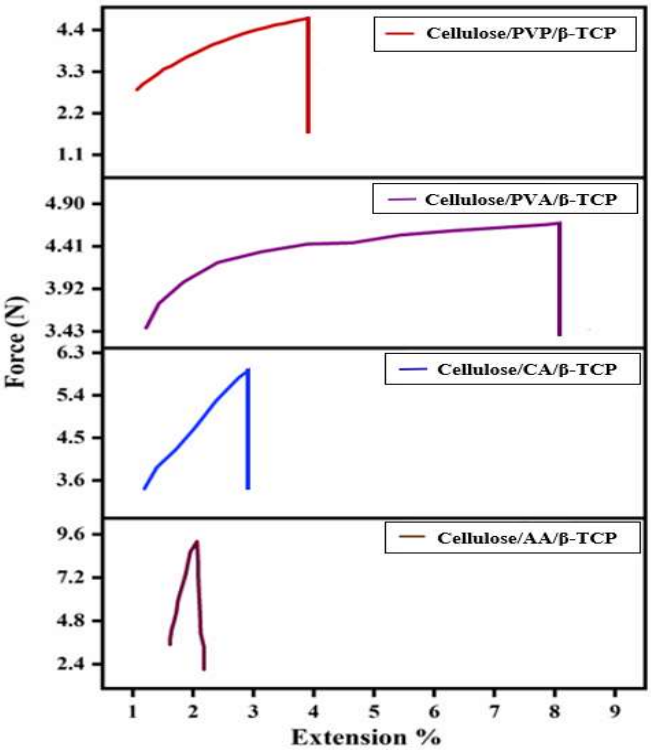

Fig. 5 UTM analysis β-TCP integrated cellulose based composites

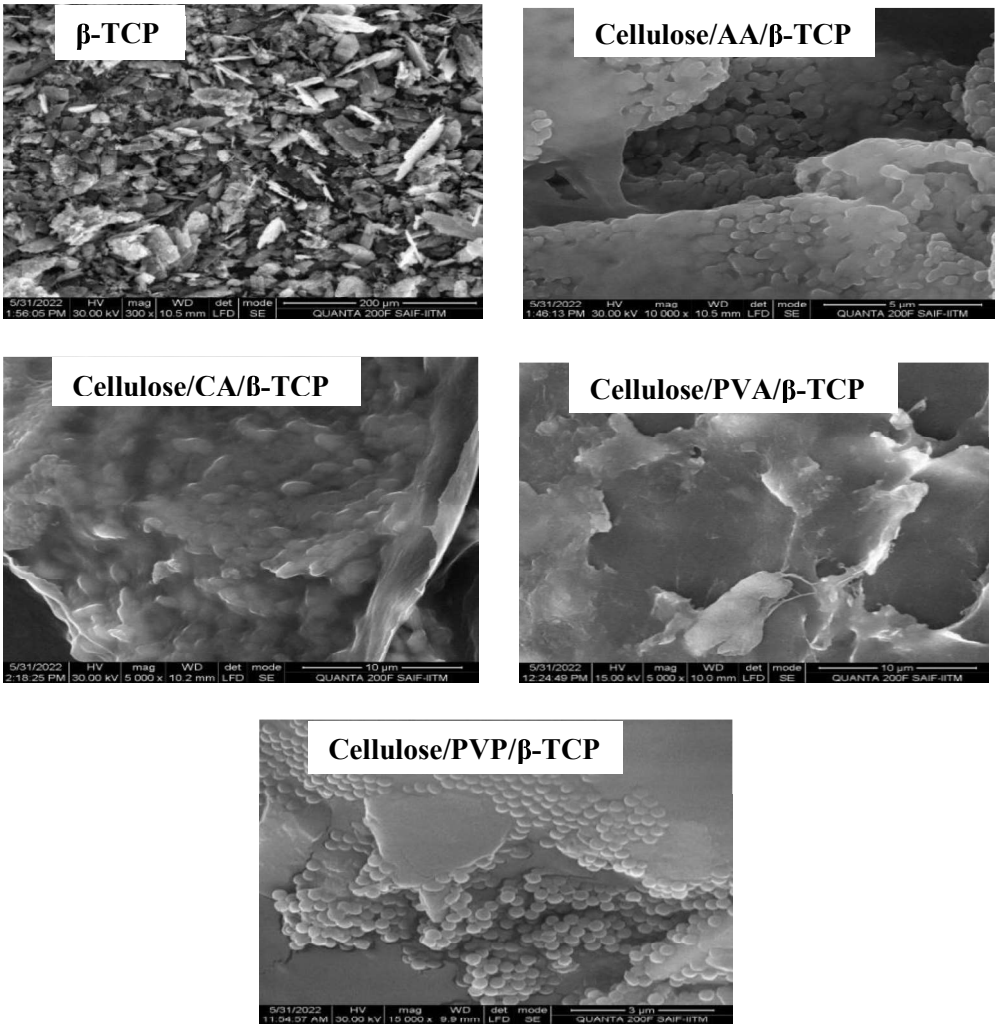

Fig. 6 SEM images of β-TCP and β-TCP integrated cellulose based composites

Fig.7 Antibacterial activity for cellulose/AA/β-TCP

Fig. 8 Antibacterial activity for cellulose/CA/β-TCP

Fig. 9 Antibacterial activity for cellulose/PVA/β-TCP

Fig. 10 Antibacterial activity for cellulose/PVP/β-TCP

Fig 11 Antifungal activity for cellulose/AA/β-TCP

Fig. 12 Antifungal activity for cellulose/CA/β-TCP

Fig. 13 Antifungal activity for cellulose/PVA/β-TCP

Fig. 14 Antifungal activity for cellulose/PVP/β-TCP

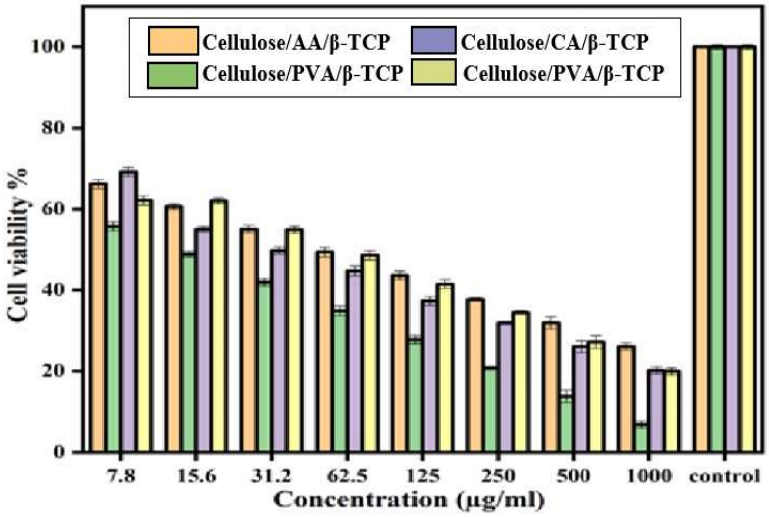

Fig. 15 Comparative cell viability % of composites

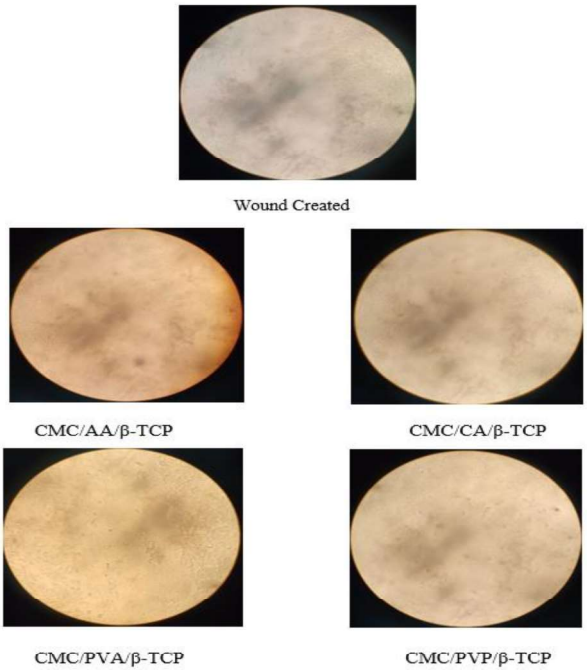

Fig. 16 Wound Healing images of β-TCP integrated cellulose based composites

Table 1 Average crystallite size, Crystallinity index, 2θ values for β-TCP and prepared Composites.

S.No	Composites	Average Crystallite Size	Crystallinity index
1	TCP	18.2nm	51.7%
2	Cellulose/AA/β-TCP	17.95 nm	46%
3	Cellulose/CA/β-TCP	16.58 nm	41.78
4	Cellulose/PVA/β-TCP	15.03 nm	40.5%
5	Cellulose/PVP/β-TCP	14.02 nm	36.15%

Table 2 Melting temperature (T_m) and decomposition temperature (T_d) for β-TCP and prepared composites

S.No	Composites	T_m (°C)	T_d (°C)
1.	Cellulose/AA/β-TCP	103°C	628°C
2.	Cellulose/CA/β-TCP	147°C	742°C
3.	Cellulose/PVA/β-TCP	160°C	572°C
4.	Cellulose/PVP/β-TCP	162°C	532°C
5.	β-TCP		730°C

Table 3 Maximum load, Tensile strength Elongation at break, Extension at maximum load, Thickness and Area of the Polymer composites.

S. No	Polymer nano composites	Maximum Load (N)	Tensile strength (MPa)	Elongation at break (%)	Extension at maximum load (mm)	Thickness (mm)	Area (mm)
1.	Cellulose/AA/β-TCP	31.57	27.27	1.67	0.50	0.11	1.3
2.	Cellulose/CA/β-TCP	35.84	17.36	3.50	1.05	0.22	2.1
3.	Cellulose/PVA/β-TCP	12.54	12.77	16.33	4.90	0.12	1.2
4.	Cellulose/PVP/β-TCP	8.95	1.57	2.00	0.60	0.55	5.6

Table 4 EDX spectra of β-TCP, Cellulose/AA/β-TCP, Cellulose/CA/β-TCP, Cellulose/PVA/β-TCP, Cellulose/PVP/β-TCP

Composites	Elements	Weight Percentage (%)	Atomic Percentage (%)
β-TCP	***C***	23.19	38.36
	O	27.84	35.05
	P	17.47	13.04
	Ca	33.68	15.55
Cellulose/AA/β-TCP	***C***	47.75	57.04
	O	36.66	34.91
	P	03.03	02.01
	S	07.76	03.19
	Ca	04.72	02.62
Cellulose/CA/β-TCP	***C***	46.18	56.71
	O	34.70	34.28
	P	03.53	02.01
	S	07.72	05.17
	Ca	05.28	02.64
Cellulose/PVA/β-TCP	***C***	37.23	53.74
	O	28.62	28.74
	P	07.05	04.37
	S	09.70	05.67
	Ca	13.85	06.55
Cellulose/PVP/β-TCP	***C***	32.23	47.70
	O	16.58	16.15
	P	04.78	03.73
	S	10.16	06.63
	Ca	11.63	03.23

Table 5 Antibacterial activity of cellulose/AA/β-TCP

Organisms	Zone of Inhibition (mm)			Antibiotic (1mg/ml)
	1000	750	500	
Staphylococcus aureus	18	17	12	20
Escherichia coli	13	11	10	13
Enterococcus fecalis	23	21	15	17
Pseudomonas aeruginosa	1	1	1	26

Table 6 Antibacterial activity of Cellulose/CA/β-TCP

Organisms	Zone of Inhibition (mm)			Antibiotic (1mg/ml)
	1000	750	500	
Staphylococcus aureus	15	15	11	17
Escherichia coli	16	16	13	21
Enterococcus fecalis	20	18	15	15
Pseudomonas aeruginosa	2	1	1	25

Table 7 Antibacterial activity of Cellulose/PVA/β-TCP

Organisms	Zone of Inhibition (mm)			Antibiotic (1mg/ml)
	1000	750	500	
Staphylococcus aureus	15	13	7	18
Escherichia coli	18	15	13	20
Enterococcus fecalis	20	20	15	15
Pseudomonas aeruginosa	1	1	1	24

Table 8 Antibacterial activity of Cellulose/PVP/β-TCP

Organisms	Zone of Inhibition (mm)			Antibiotic (1mg/ml)
	1000	750	500	
Staphylococcus aureus	16	14	9	19
Escherichia coli	17	15	13	19
Enterococcus fecalis	24	21	17	17
Pseudomonas aeruginosa	1	1	1	27

Table 9 Antifungal activity of cellulose/AA/β-TCP

Organisms	Zone of Inhibition (mm)			Antibiotic (1mg/ml)
	Sample (µg/ml)			
	1000	750	500	
Trichoderma viride	40	31	21	37
Rhizopus sp.	11	09	1	10
Candida albicans	35	13	11	37

Table 10 Antifungal activity of cellulose/CA/β-TCP

Organisms	Zone of Inhibition (mm)			Antibiotic (1mg/ml)
	Sample (µg/ml)			
	1000	750	500	
Trichoderma viride	33	27	26	40
Rhizopus sp	12	06	1	14
Candida albicans	33	23	12	24

Table 11 Antifungal activity of Cellulose/PVA/β-TCP

Organisms	Zone of Inhibition (mm)			Antibiotic (1mg/ml)
	Sample (µg/ml)			
	1000	750	500	
Trichoderma viride	31	20	08	33
Rhizopus sp.	10	07	1	13
Candida albicans	30	20	13	30

Table 12 Antifungal activity of cellulose/PVP/β-TCP

Organisms	Zone of Inhibition (mm)			Antibiotic (1mg/ml)
	Sample (µg/ml)			
	1000	750	500	
Trichoderma viride	33	25	14	37
Rhizopus sp.	09	1	1	11
Candida albicans	31	26	13	34

Table 13 Wound closure % of the composites

S.No	Composites	Wound created (before)	After	Wound closure %
1.	Cellulose/AA/β-TCP	5.16mm	3.16mm	35.8%
2.	Cellulose/CA/β-TCP	5.16mm	3.29mm	41.02%
3.	Cellulose/PVA/β-TCP	5.16mm	2.42mm	46.30%
4.	Cellulose/PVP/β-TCP	5.16mm	2.73mm	41.73%

References

1. T. P. Sathishkumar, L. Rajeshkumar, G. Rajeshkumar, M. R. Sanjay, S. Siengchin , N.Thakrishnan , E3S Web of Confe. 355, 02006, 2022.
2. P. Madhu, M. R. Sanjay P., Senthamaraikannan , S. Pradeep, S. S. Saravanakumar, B.Yogesha, J Nat Fibers. 16, 1132, 2018.
3. T. Rohan,B. Tushar, G.,T. Mahesha, IOP Conf Series Mater Sci Eng. 314, 012020, 2018.
4. T.Y.Gowda, M. R. Sanjay, K.S. Bhat, P.Madhu ,P. Senthamaraikannan, B.Yogesha, Cogent Eng. 5, 1446667, 2018.
5. B. T. Narendiranath, S.S.Aravind , Kumar KSN, Rao MSS. Int J Mech Eng Technol. 9, 11, 2018.
6. M. R. Sanjay, G. R.Arpitha, L .L. Naik, K. Gopalakrishna, B. Yogesha, Nat Resour. 7, 2108, 2016.
7. R.S. Rana, R. Purohit, Mater Today Proc. 4, 3466, 2017.
8. Y. Swolfs, L. Gorbatikh , I. Verpoest Appl Sci Manuf. 67, 181, 2014.
9. M.T. Hayajneh, M.M.Al-Shrida, F.M.AL-Oqla, e-Polymers., 22, 641, 2022
10. V. Dhawan, S. Singh, I. Singh, J Compos. 7, 792620, 2013.
11. E. Habib, R. Wang, Y.Wang, M. Zhu , X.X. Zhu. ACS Biomater Sci Eng. 2, 1, 2016.
12. M. T. Hayajneh, F.M. AL-Oqla, M .M. Al-Shrida, e-Polymers. 21, 710, 2021.
13. M. Ramesh, L .Rajeshkumar, V. Bhuvaneswari, Emergent Mater. 5, 833, 2021.
14. D. Balaji, M. Ramesh, T. Kannan, S. Deepan V., Bhuvaneswari, L.Rajeshkumar Mater Today Proc. 42, 350, 2021.

15. de Araujo Alves Lima R, Kawasaki Cavalcanti D, de Souza e Silva Neto J, Meneses da Costa H, Banea MD. Polym Compos. 41, 314, 2020.
16. S. B. R.Devireddy, S.Biswas , Polym Compos. 38, 1396, 2017
17. Salama, International Journal of Biological Macromolecules, 127, 606, 2019
18. A. Allwyn Sundar Raj, T.V. Ranganathan, J. of Pharmacy Res., 9, 4309, 2018.
19. T.S. Kiruthika, E.K.T. Sivakumar, V. Jaisankar, Asian J. of Chem., 34, 2022, 2843.
20. H. Chaair, H. Labjar, O. Britel, Synthesis of β-tricalcium phosphate, Morphologie, 313, 2017.
21. M. Sasikala,, and M. J. Umapathy, New Journal of Chemistry, 42.24, 19979, 2018.
22. Kumar, Anuj, Y. S. Negi, N. K. Bhardwaj, and V. Choudhary, Advanced Materials Letters, 4.8, 626, 2013
23. Liu, Liying, Rui Cai, Yejing Wang, Gang Tao, Lisha Ai, Peng Wang, and others, International Journal of Molecular Sciences, 19.10, 2018.
24. S. Maheshwari, K.Uma, M. Govindan, A. Raja,.M. Raja, B.S. Pravin, and S. Vasanth Kumar, Bio-Medical Materials and Engineering, 28.4, 401, 2017.
25. M. Hiljanen-Vainio, M.Heino , J.V. Sepp.al. Polymer, 39, 865, 1998.